Clinical Application of Liver MR Imaging in Wilson's Disease

Jung-Eun Cheon, MD[1]
In-One Kim, MD[1]
Jeong Kee Seo, MD[2]
Jae Sung Ko, MD[2]
Jeong Min Lee, MD[1]
Cheong-Il Shin, MD[1]
Woo Sun Kim, MD[1]
Kyung Mo Yeon, MD[1]

Index terms:
Hepatolenticular degeneration
Liver
Magnetic resonance (MR)

DOI:10.3348/kjr.2010.11.6.665

Korean J Radiol 2010;11:665-672
Received January 22, 2010; accepted after revision July 8, 2010.

[1]Department of Radiology, Seoul National University College of Medicine, and the Institute of Radiation Medicine, SNUMRC, Seoul 110-744, Korea; [2]Department of Pediatrics, Seoul National University College of Medicine, Seoul 110-744, Korea

Corresponding author:
In-One Kim, MD, Department of Radiology, Seoul National University College of Medicine, 101 Daehangno, Jongno-gu, Seoul 110-744, Korea.
Tel. (822) 2072-3608
Fax. (822) 747-5781
e-mail: kimio@radcom.snu.ac.kr

Objective: To determine whether there is a correlation between liver MR findings and the clinical manifestations and severity of liver dysfunction in patients with Wilson's disease.

Materials and Methods: Two radiologists retrospectively evaluated MR images of the liver in 50 patients with Wilson's disease. The Institutional Review Board approved this retrospective study and informed consent was waived. MR images were evaluated with a focus on hepatic contour abnormalities and the presence of intrahepatic nodules. By using Fisher's exact test, MR findings were compared with clinical presentations (neurological and non-neurological) and hepatic dysfunction, which was categorized by the Child-Pugh classification system (A, B and C). Follow-up MR images were available for 17 patients.

Results: Contour abnormalities of the liver and intrahepatic nodules were observed in 31 patients (62%) and 25 patients (50%), respectively. Each MR finding showed a statistically significant difference ($p < 0.05$) among the three groups of Child-Pugh classifications (A, n = 36; B, n = 5; C, n = 9), except for splenomegaly ($p = 0.243$). The mean age of the patients with positive MR findings was higher than that of patients with negative MR findings. For patients with Child-Pugh class A (n = 36) with neurological presentation, intrahepatic nodules, surface nodularity, and gallbladder fossa widening were more common. Intrahepatic nodules were improved (n = 8, 47%), stationary (n = 5, 29%), or aggravated (n = 4, 24%) on follow-up MR images.

Conclusion: MR imaging demonstrates the contour abnormalities and parenchymal nodules of the liver in more than half of the patients with Wilson's disease, which correlates with the severity of hepatic dysfunction and clinical manifestations.

Wilson's disease or progressive hepatolenticular degeneration is an autosomal recessive disorder of copper metabolism (1). The gene that causes Wilson's disease, located at chromosome 13 band q14.3, is known to code for a copper-transporting P-type ATPase (2–4). A mutation of the gene associated with Wilson's disease results in deficient biliary excretion of copper, leading to excessive copper accumulation in many tissues. Copper accumulation occurs mainly in the liver, but also in the brain, cornea, and kidney (1–5). The principal clinical manifestations of Wilson's disease are either hepatic or neurological disease (6, 7).

Ultrasound (US), CT, and MR findings of the liver in Wilson's disease usually reflect nonspecific hepatic injury including fatty infiltration, acute hepatitis, chronic active hepatitis, and cirrhosis (8–12). In advanced Wilson's disease, nodular infiltrations suggesting the presence of copper-containing nodules and contour abnormalities consis-

tent with cirrhosis have been reported in the literature (12–14). However, the clinical applications of MR imaging features of the liver in Wilson's disease have not yet been established. The purpose of this study was to evaluate the morphological features of the liver on MR images obtained in patients with Wilson's disease, and determine whether there is a correlation between the MR findings and clinical manifestations and severity of hepatic dysfunction.

MATERIALS AND METHODS

Patients

MR images of the liver were retrospectively reviewed alongside clinical findings in 50 children and young adults with Wilson's disease (M:F = 33:17; age range, 5–26 years; median age, 14 years). The database of the computed hospital information system was cross-referenced with the MR imaging database to identify all patients with Wilson's disease who had undergone MR imaging of the liver at the institution over the course of a 10-year period from January 1997 to January 2007. The institutional review board approved the review of the radiological and clinical data for this study and waived the requirement for patient informed consent. Wilson's disease was diagnosed based on a combination of low serum ceruloplasmin levels accompanied with elevated 24-hour urinary copper excretion (n = 50), as well as the presence of a Kayser-Fleischer (K-F) ring (n = 28), and a liver biopsy (n = 12).

Patients were classified at the time of diagnosis as having neurological (either current clinical or historical evidence of neurological dysfunction which was not associated with symptomatic liver disease) and non-neurological presentation, including hepatic (an increase in serum transaminase levels, acute/chronic hepatitis or cirrhosis) and asymptomatic presentation (siblings of index cases with no disease-related symptoms) (6). The hepatic function of the each patient was categorized into three groups (class A, B and C) according to the Child-Turcotte-Pugh score (5 to 15-point scale) (15).

Twenty-two patients had been treated with copper chelators, D-penicillamine (n = 16), or trientine (n = 6) (median duration of treatment: 6 years, range: 0.5–12 years) at the time of MR imaging. Another 28 patients were diagnosed with Wilson's disease at the time of MR imaging and was administered any copper chelating agents. The clinical characteristics of the patients were summarized in Table 1. All patients were followed at the pediatric outpatient clinic, and follow-up MR images were available for 17 patients.

MR Imaging

All examinations were obtained using 1.0 or 1.5 Tesla MR scanners (Siemens Medical Systems, Erlangen, Germany). This retrospective data collection was preceded by the various MR imaging protocols for the liver. However, the studies included the following MR sequences: an axial T2-weighted fast spin-echo sequence (repetition time msec/echo time msec, 3500–5000/96–144) and an axial T1-weighted spin echo sequence (repetition time msec/echo time msec, 410–530/1.5–2.2) with a 7 mm thickness, 1–2-mm gap, 256 × 256 matrix size and field-of-view, 240 × 320.

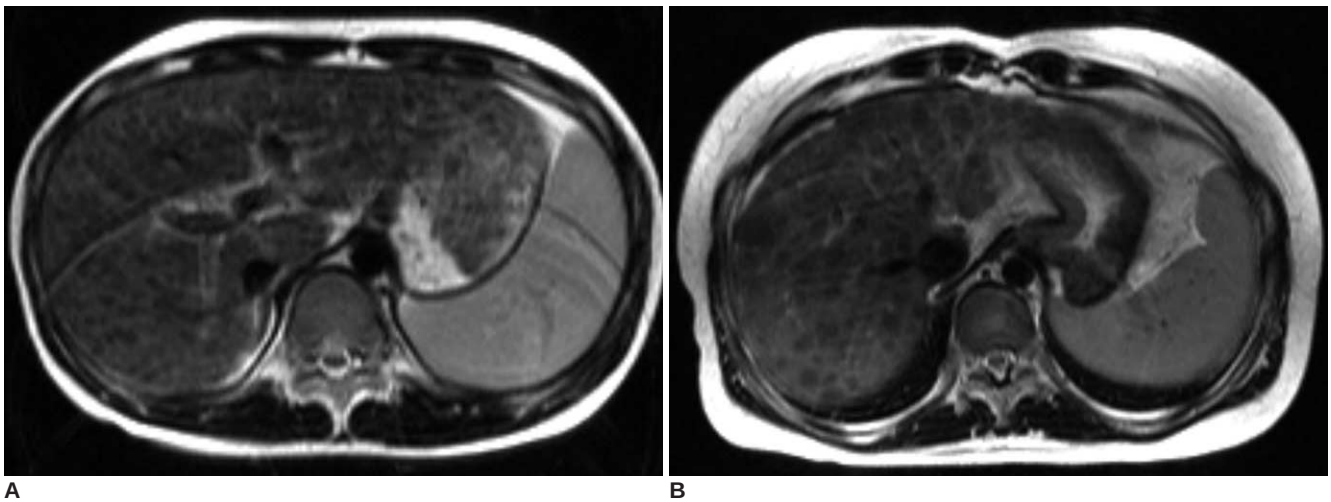

A B

Fig. 1. Interpretation of intrahepatic nodules in Wilson's disease on T2-weighted images (TR/TE = 3500/100)
A. 9-year-old girl with Wilson's disease and elevated liver enzymes (Child-Pugh class A) shows innumerable tiny, hypointense nodules (≤ 3 mm in diameter, grade 1) in liver on T2-weighted image.
B. 24-year-old woman with Wilson's disease who presented with jaundice (Child-Pugh class B) shows innumerable hypointense nodules (> 3 mm in diameter, grade 2) on T2-weighted image.

MR Imaging Analysis

Two radiologists, each with more than seven years of experience in MR body imaging, retrospectively evaluated the MR images. The radiologists were blinded to the clinical and pathological findings. The two readers evaluated the MR images for (a) the presence and pattern of intrahepatic nodules, (b) the contour abnormalities of the liver and (c) additional findings such as a gallbladder abnormality, splenomegaly, venous collateral formation, or ascites.

A three-point scoring system was used to evaluate the pattern of intrahepatic nodules as follows: 0 for none, 1 for granular ($\leq$ 3 mm in diameter), and 2 for macronodular ($>$ 3 mm in diameter) (Fig. 1). We evaluated the signal intensity of the nodules on T1-weighted images in comparison to the underlying liver parenchyma. The various contour abnormalities of the liver identified included surface nodularity, gallbladder fossa widening, and caudate hypertrophy. Surface nodularity of the liver and the gallbladder fossa widening were assessed subjectively by the evaluation of irregularities along the liver surface and enlargement of the pericholecystic space (i.e., the gallbladder fossa), respectively. Caudate hypertrophy was evaluated using a modified caudate-right lobe ratio (16).

Twenty follow-up MR examinations obtained from 17 patients over a 10-year period (mean interval 28 months, range, 8–130 months) were also evaluated with the same MR interpretation protocols. Nine patients underwent MR imaging, before and after treatment, using copper chelating agents. In the eight remaining patients, both initial and follow-up MR examinations were obtained during treatment with copper chelating agents.

Table 1. Clinical Characteristics of 50 Patients with Wilson's Disease

	Clinical Presentation		
	Neurological (n = 12)	Non-Neurological (n = 38)	*P* value
Male/female ratio	7:5	26:12	0.728
Age (years)			
at diagnosis	13.8±1.9	11.9±5.9	0.093
at MR examination	14.6±2.3	13.6±6.2	0.539
Kayser-Fleischer ring	11 (92%)	17 (45%)	0.006
Hepatic Function			0.048
Child-Pugh class A	12 (100%)	24 (63%)	
Child-Pugh class B	0	5 (13%)	
Child-Pugh class C	0	9 (24%)	
Treatment			
Untreated/treated	7:5	21:17	0.852
Duration of treatment (years)	2.8±1.8	6.2±3.8	0.120

Statistical Analysis

The prevalence of the MR imaging findings was estimated as a percentage of the patients displaying each abnormality. The overall association between the MR findings and clinical presentations (neurological or non-neurological), or severity of hepatic dysfunction (Child-Pugh classification A, B, C), was assessed with a contingency table, employing the Chi-squared and Fisher's exact tests. The association of clinical features for both clinical presentations was also evaluated by Chi-squared and Fisher's exact probability tests. Differences in age and duration of treatment were compared for both groups of

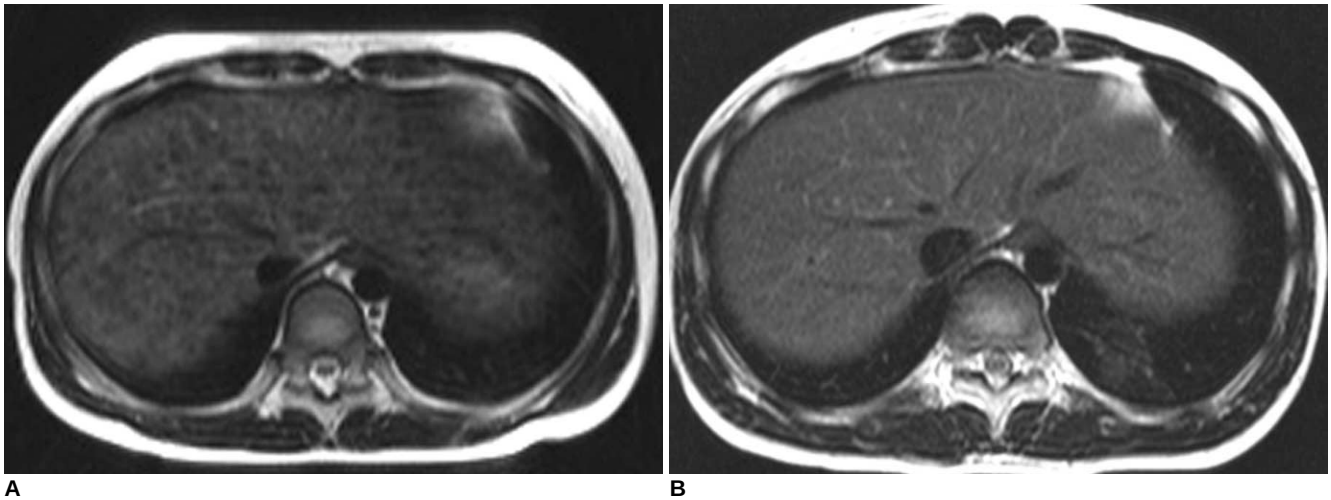

A **B**

Fig. 2. 11-year-old girl diagnosed with Wilson's disease (Child-Pugh class A).
A. T2-weighted axial image shows multiple small hypointense nodules ($\leq$ 3 mm in diameter, grade 1) in liver.
B. Follow-up T2-weighted axial image obtained 18 months after D-penicillamine treatment shows near disappearance of hypointense nodules in liver.

clinical presentation, three groups of hepatic dysfunction, and type of MR finding using non-parametric probability tests (Mann-Whitney or Kruskal-Wallis). All *p*-values were based on two tailed comparisons and a 5% confidence-level was considered to indicate a statistically significant difference. Statistical analyses were performed with SPSS 7.5 for Windows (SPSS, Chicago, IL).

RESULTS

Clinical Features

At the time of diagnosis, 12 patients presented with neurological dysfunction, compared to 38 patients who presented with non-neurological manifestations (33 patients with hepatic dysfunction and five asymptomatic siblings of index cases). The K-F ring was most common in the neurological presentation (92%, 11 of 12) relative to non-neurological presentation (45%; 17 of 38; $p = 0.006$). There were no statistically significant differences between sex, age, presence of medical treatment, and duration of treatment among both clinical presentations (Table 1).

Patient hepatic function was categorized as Child-Pugh class A in 36 patients, Child-Pugh class B in five patients, and Child-Pugh class C in nine patients. Mean age at diagnosis was 11.1 years in class A, 13.4 years in class B, and 17.0 years in class C. A statistically significant differ-

Table 2. Association Between Liver MR Imaging and Hepatic Dysfunction

Liver MR Findings	No. of Patients	Child-Pugh Classification			*P* value
		A (n = 36)	B (n = 5)	C (n = 9)	
Intrahepatic nodule					
Hypointense nodules on T2WI	25 (50%)	12 (33%)	5 (100%)	8 (89%)	< 0.001
Grade 1	13 (26%)	9 (25%)	2 (40%)	2 (22%)	
Grade 2	12 (24%)	3 (8%)	3 (60%)	6 (67%)	
Hyperintense nodules on T1WI	14 (28%)	6 (17%)	4 (80%)	4 (44%)	0.004
Hepatic Contour					
Surface nodularity	25 (50%)	13 (36%)	4 (80%)	8 (89%)	0.006
Caudate hypertrophy	10 (20%)	2 (6%)	3 (60%)	5 (56%)	< 0.001
Gallbladder fossa widening	29 (58%)	17 (47%)	5 (100%)	7 (78%)	0.031
Others					
Ascites	7 (14%)	1 (3%)	1 (20%)	5 (56%)	0.001
Venous collaterals	10 (20%)	3 (8%)	1 (20%)	6 (67%)	0.012
Gallbladder wall edema	12 (24%)	2 (6%)	3 (60%)	7 (78%)	< 0.001
Splenomegaly	40 (80%)	27 (75%)	4 (80%)	9 (100%)	0.243

Note.— Grade 1 = granular nodules (≤ 3 mm in diameter), Grade 2 = macronodular lesions (> 3 mm in diameter), SI = signal intensity, T1WI = T1-weighted images, T2WI = T2-weighted images

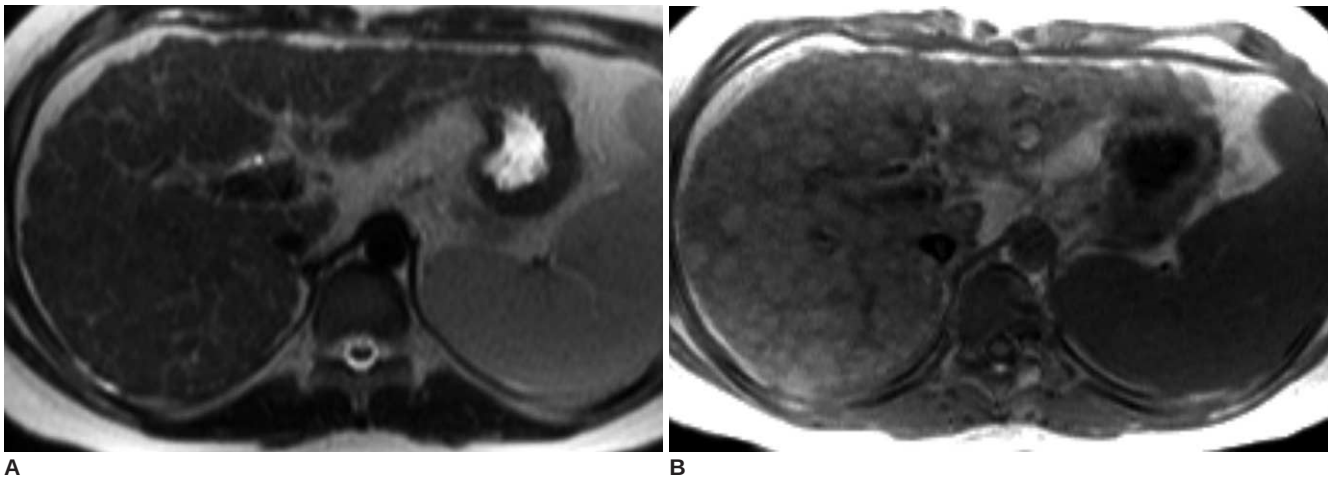

A **B**

Fig. 3. 11-year-old boy with Wilson's disease (Child-Pugh class B)
A. T2-weighted image shows mild irregularity of liver surface and multiple, hypointense nodules in liver.
B. These macronodular lesions show hyperintensities on T1-weighted images.

ence was noted for age at MR imaging among the three groups of Child-Pugh classification ($p = 0.036$). All of the patients with a neurological presentation were categorized as class A. Another 38 patients with non-neurological presentation were categorized as class A (n = 24, 63%), class B (n = 5, 13%), and class C (n = 9, 24%). There was a statistically significant difference for Child-Pugh classification between neurological and non-neurological presentations ($p = 0.048$). The clinical findings of 50 patients are summarized in Table 1.

MR Imaging Findings

Twenty-five patients (50%) demonstrated hypointense hepatic nodules on T2-weighted images. The nodules were granular (grade 1, $\leq$ 3 mm in diameter) in 13 patients (Figs. 1A, 2A), or macronodular (grade 2, > 3 mm in diameter) in 12 patients (Figs. 1B, 3A, 4A). These nodules were hyperintense (n = 14) or isointense, or slightly hypointense (n = 11) as seen on T1-weighted images (Figs. 3B, 4B). Thirty-one patients (62%) showed contour abnormalities such as surface nodularity (n = 25), caudate hypertrophy (n = 10), or gallbladder fossa widening (n = 29) (Figs. 3, 4). Ascites, venous collaterals, and splenomegaly were observed in seven patients, 10 patients, and 40 patients, respectively. Edematous wall thickening of the gallbladder was observed in 12 patients, and a gallbladder stone or sludge in three patients (Fig. 4).

Clinical Correlation of MR Imaging Findings

In the 36 patients belonging to Child-Pugh class A, hypointense nodules as seen on T2-weighted images, were detected in 12 patients (33%) (grade 1 [n = 9, 25%] and grade 2 [n = 3, 8%]). Contour abnormalities of the liver were noted in 17 patients (47%). In the five patients categorized as Child-Pugh class B, hypointense nodules as seen on T2-weighted images, and contour abnormalities of the liver were detected in all patients. Macronodular lesions (grade 2, > 3 mm in diameter) were observed in three patients (60%) (Fig. 3). In the nine patients categorized as Child-Pugh class C, hypointense nodules as seen on T2-weighted images and contour abnormalities of the liver were noted in all patients except for one (89%).

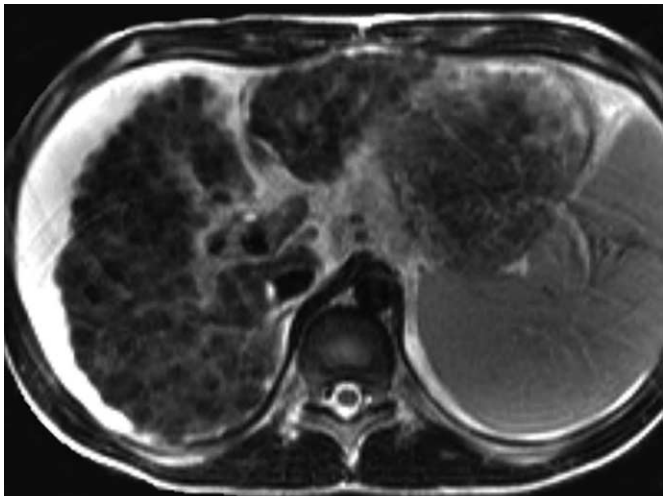

A

B

C

Fig. 4. 24-year-old man with Wilson's disease and advanced cirrhosis (Child-Pugh class C).
A. Disseminated hyperintense nodules greater than 1 cm in size relative to liver parenchyma are seen on axial T2-weighted MR image. Note surface irregularity and parenchymal contraction of liver.
B. T1-weighted axial image of liver shows multiple hyperintense nodules. Gallbladder stone (arrow) is seen as nodular hyperintensity near porta hepatis.
C. Harvested liver during liver transplantation shows macronodular cirrhosis. There was no evidence of hepatocellular carcinoma.

Table 3. Association of Liver MR Imaging and Age at MR Examination

Liver MR Findings	Mean Age (± Standard Deviation)		
	Positive	Negative	*P* value
Intrahepatic nodule			
Hypointense nodules on T2WI	15.8 ± 4.6	11.9 ± 5.8	0.001
Hyperintense nodules on T1WI	16.1 ± 5.4	12.9 ± 5.4	0.113
Hepatic Contour			
Surface nodularity	16.4 ± 4.8	11.2 ± 5.1	< 0.001
Caudate hypertrophy	19.5 ± 3.8	12.4 ± 5.0	< 0.001
Gallbladder fossa widening	16.2 ± 4.6	10.6 ± 5.1	0.001
Others			
Ascites	20.3 ± 6.7	12.8 ± 4.6	0.006
Venous collaterals	18.6 ± 6.4	12.7 ± 4.9	0.013
Gallbladder wall edema	17.6 ± 6.4	12.6 ± 4.7	0.025
Splenomegaly	15.2 ± 5.1	8.4 ± 3.8	< 0.001

Table 4. Association of Liver MR Imaging and various Clinical Manifestations

Liver MR Findings in Patients with Child-Pugh Class A (n = 36)	Clinical Presentation		*P* value
	Neurological (n = 12)	Non-Neurological (n = 24)	
Intrahepatic nodules			
Hypointensity on T2WI	8 (67%)	4 (17%)	0.007
Hyperintense on T1WI	4 (33%)	2 (8%)	0.149
Hepatic Contour			
Surface nodularity	8 (67%)	5 (21%)	0.011
Caudate hypertrophy	0	2 (8%)	0.543
Gallbladder fossa widening	11 (92%)	6 (25%)	< 0.001
Others			
Ascites	0	1 (4%)	1.000
Venous collaterals	1 (8%)	2 (8%)	1.000
Gallbladder wall edema	0	2 (8%)	0.543
Splenomegaly	11 (92%)	16 (67%)	0.108

Macronodular lesions were observed in six patients (67%) (Fig. 4). Each MR imaging finding demonstrated a statistically significant difference among the three groups of Child-Pugh classification except for splenomegaly (p = 0.243). A summary of the MR findings and association of MR findings with the severity of hepatic dysfunction are listed in Table 2. For each MR imaging finding, mean age at MR examination was greater in patients with a positive finding than those with negative findings, and were statistically significant except in hyperintense nodules on T1-weighted images (p = 0.113) (Table 3).

In the patients belonging to Child-Pugh class A (n = 36), MR findings such as intrahepatic nodules (p = 0.007), surface nodularity (p = 0.011), and gallbladder fossa widening (p < 0.001) demonstrated a statistically significant difference between patients with neurological presentation and non-neurological presentation. Other MR findings did not present a statistically significant difference between neurological presentation and non-neurological presentation (Table 4).

Follow-Up MR Imaging Findings and Clinical Features

Twenty follow-up MR examinations obtained from 17 patients demonstrated improved hepatic nodular infiltrations for eight patients, aggravated intrahepatic nodules and/or cirrhosis for four patients, and a stationary state of imaging features for five patients (Fig. 2B). In the eight patients with improved nodular lesions, all of them showed improved hepatic dysfunction (normalized serum transaminase level, n = 5; improved hyperbilirubinemia, n = 1; improved coagulation abnormality, n = 2). In four patients with aggravated nodular lesions and/or cirrhosis, newly appeared intrahepatic nodules were detected in two patients, whereas aggravated intrahepatic nodules and cirrhosis were observed in two patients. Among these four patients, two patients underwent liver transplantation (Fig. 4C).

DISCUSSION

In Wilson's disease, asymptomatic hepatic copper deposition in liver cells occurs early in the disease's progression, predominantly in the periportal regions and along the hepatic sinusoids (17, 18). After episodes of acute hepatitis, which may be reflected by elevated plasma levels of liver enzymes, a fatty change and periportal inflammation can develop. Afterwards, piecemeal necrosis and fibrosis with inflammatory cell infiltrations induce chronic active hepatitis. Finally, after several years, insidious development of irreversible cirrhosis occurs (19). In a large cohort study of patients with Wilson's disease, liver biopsies revealed variable hepatic involvement in 37% of patients presenting cirrhosis, 36% at an unspecified stage of fibrosis, and 54% with steatosis (20).

Considering the variable hepatic involvement, various imaging findings of the liver in Wilson's disease are demonstrated (8–13). Recently, Akhan et al. (14) reported that Wilson's disease should be considered as one of the leading diagnoses of young patients with a perihepatic fat

layer, parenchymal heterogeneity with multiple nodules, and the absence of caudate lobe hypertrophy. It also suggested that US seemed to be the best imaging modality for the demonstration of early parenchymal alteration. In this study, hypointense nodules on T2-weighted images, surface nodularity of the liver, and gallbladder fossa widening were common MR imaging findings in patients with Wilson's disease, and these correlated with severity of hepatic dysfunction. Among the patients with normal or mild hepatic dysfunction (Child-Pugh class A), the MR findings were more common in patients with the neurological manifestations than the non-neurological manifestations of Wilson's disease. Therefore, it is postulated that neurological dysfunction, which was not associated with symptomatic liver disease, might be related with hepatic copper accumulation and subsequent hepatic parenchymal changes.

Hepatic nodules in Wilson's disease are considered as a result of copper deposition. On MR imaging, these lesions typically appear as hypointense on T2-weighted images and hyperintense on T1-weigthed images (9, 14). In this study, multiple hypointense nodules were commonly noted on T2-weighted images (50%). The paramagnetic effect of ionic copper has been implicated as a cause of hypointensity, as was observed on T2-weighted images and hyperintensity as observed on T1-weighted images. However, the T1-shortening and T2-shortening effect of copper deposition may be nullified by elevated T1 and T2 values in advanced cirrhosis (17). Multiple hypoinstense nodules of the liver were noted in 33% of patients with early stage of hepatic dysfunction (Child-Pugh class A) before advanced cirrhosis. In patients with advanced hepatic dysfunction (Child-Pugh classes B and C), hypointense nodules of the liver were noted in 93% (13 of 14) of the patients and 50% of the nodules were macronodular (> 3 mm in diameter) and were observed as hyperintense on T1-weighted images.

Contour abnormalities of the liver due to parenchymal necrosis, regeneration, and scarring that suggest cirrhosis were correlated with hepatic dysfunction in this study. The expanded gallbladder fossa sign has been reported to be a highly specific MR sign for the diagnosis of cirrhosis, and consists of the enlargement of the pericholecystic space (i.e., the gallbladder fossa) (21). This is comparable to the finding of a thickened perihepatic fat layer as described by Akhan et al. (10). A normal caudate to right lobe ratio has been reported as a unique feature of cirrhosis in Wilson's disease (14). In this study, caudate hypertrophy was less common (20% of patients) relative to other imaging features that were suggestive of cirrhosis. However, an explanation is not postulated for the mechanism of lobar dysmorphism of the liver in these patients.

Reversibility of copper deposition after copper chelating therapy is noteworthy. Kim et al. (22) reported that MR imaging of the brain depicts the reversible changes of the involved brain parenchyma after copper chelating therapy. Reversible changes of copper deposition in the liver have been rarely reported (12, 14, 23). In this study, follow-up MR images of the liver demonstrated improved intrahepatic nodules in 47% (8 of 17) of patients after copper chelating therapy with clinical improvement of liver function. Follow-up MR examinations also demonstrated aggravated nodular infiltrations and progressed contour abnormalities of cirrhosis in four patients with rapidly progressive hepatic dysfunction. From this point of view, MR imaging may be used as an indicator of therapeutic response in Wilson's disease.

This study has several limitations. First, clinical grading of Wilson's disease has not yet been fully established. The Child-Pugh classification was used in the evaluation of clinical status of Wilson's disease, which only reflects hepatic dysfunction. Serum ceruloplasmin and copper levels, as well as the 24-hour urinary copper level were not considered. Although 50 patients with Wilson's disease were included in the study, most of the patients were Child-Pugh class A, and only 25% of the patients were Child-Pugh class B or C. Therefore, an error in the statistical analysis was inevitable. Second, the MR protocol could not be uniformly assumed, as the study included retrospective data collection for a 10-year span. Third, interobserver or intraobserver variance analyses were not performed for the MR imaging interpretation.

In conclusion, MR imaging of the liver in Wilson's disease demonstrated multiple, hypointense nodules on T2-weighted images, as well as contour abnormalities of the liver suggestive of cirrhosis. These imaging features correlated with the severity of hepatic dysfunction and clinical presentation. MR imaging also demonstrated reversible parenchymal changes after clinical improvement.

References

1. Gitlin JD. Wilson disease. *Gastroenterology* 2003;125:1868-1877
2. Bull PC, Thomas GR, Rommens JM, Forbes JR, Cox DW. The Wilson disease gene is a putative copper transporting P-type ATPase similar to the Menkes gene. *Nat Genet* 1993;5:327-337
3. Tanzi RE, Petrukhin K, Chernov I, Pellequer JL, Wasco W, Ross B, et al. The Wilson disease gene is a copper transporting ATPase with homology to the Menkes disease gene. *Nat Genet* 1993;5:344-350
4. Seo JK. Wilson disease: an update. *Korean J Hepatol* 2006;12:333-363 [Korean]
5. Ala A, Schilsky ML. Wilson disease: pathophysiology, diagnosis,

treatment, and screening. *Clin Liver Dis* 2004;8:787-805
6. Ferenci P, Caca K, Loudianos G, Mieli-Vergani G, Tanner S, Sternlieb I, et al. Diagnosis and phenotypic classification of Wilson disease. *Liver Int* 2003;23:139-142
7. Panagiotakaki E, Tzetis M, Manolaki N, Loudianos G, Papatheodorou A, Manesis E, et al. Genotype-phenotype correlations for a wide spectrum of mutations in the Wilson disease gene (ATP7B). *Am J Med Genet A* 2004;131:168-173
8. Cançado EL, Rocha Mde S, Barbosa ER, Scaff M, Cerri GG, Magalhães A, et al. Abdominal ultrasonography in hepatolenticular degeneration. A study of 33 patients. *Arq Neuropsiquiatr* 1987;45:131-136
9. Ko S, Lee T, Ng S, Lin J, Cheng Y. Unusual liver MR findings of Wilson's disease in an asymptomatic 2-year-old girl. *Abdom Imaging* 1998;23:56-59
10. Akhan O, Akpinar E, Oto A, Köroglu M, Ozmen MN, Akata D, et al. Unusual imaging findings in Wilson's disease. *Eur Radiol* 2002;12:S66-S69
11. Chu WC, Leung TF, Chan KF, Yeung DK, Yeung TK, Cheung HM, et al. Wilson's disease with chronic active hepatitis: monitoring by in vivo 31-phosphorus MR spectroscopy before and after medical treatment. *AJR Am J Roentgenol* 2004;183:1339-1342
12. Kozic D, Svetel M, Petrovic I, Sener RN, Kostic VS. Regression of nodular liver lesions in Wilson's disease. *Acta Radiol* 2006;47:624-627
13. Akpinar E, Akhan O. Liver imaging findings of Wilson's disease. *Eur J Radiol* 2007;61:25-32
14. Akhan O, Akpinar E, Karcaaltincaba M, Haliloglu M, Akata D, Karaosmanoglu AD, et al. Imaging findings of liver involvement of Wilson's disease. *Eur J Radiol* 2009;69:147-155
15. Child CG, Turcotte JG. *Surgery and portal hypertension*. In: Child CG, ed. *The liver and portal hypertension*. Philadelphia, PA: Saunders, 1964:50-52
16. Awaya H, Mitchell DG, Kamishima T, Holland G, Ito K, Matsumoto T. Cirrhosis: modified caudate-right lobe ratio. *Radiology* 2002;224:769-774
17. Mergo PJ, Ros PR, Buetow PC, Buck JL. Diffuse disease of the liver: radiologic-pathologic correlation. *Radiographics* 1994;14:1291-1307
18. Davies SE, Williams R, Portmann B. Hepatic morphology and histochemistry of Wilson's disease presenting as fulminant hepatic failure: a study of 11 cases. *Histopathology* 1989;15:385-394
19. Cope-Yokoyama S, Finegold MJ, Sturniolo GC, Kim K, Mescoli C, Rugge M, et al. Wilson disease: histopathological correlations with treatment on follow-up liver biopsies. *World J Gastroenterol* 2010;16:1487-1494
20. Merle U, Schaefer M, Ferenci P, Stremmel W. Clinical presentation, diagnosis and long-term outcome of Wilson's disease: a cohort study. *Gut* 2007;56:115-120
21. Ito K, Mitchell DG, Gabata T, Hussain SM. Expanded gallbladder fossa: simple MR imaging sign of cirrhosis. *Radiology* 1999;211:723-726
22. Kim TJ, Kim IO, Kim WS, Cheon JE, Moon SG, Kwon JW, et al. MR imaging of the brain in Wilson disease of childhood: findings before and after treatment with clinical correlation. *AJNR Am J Neuroradiol* 2006;27:1373-1378
23. Taly AB, Meenakshi-Sundaram S, Sinha S, Swamy HS, Arunodaya GR. Wilson disease: description of 282 patients evaluated over 3 decades. *Medicine (Baltimore)* 2007;86:112-121